Experimental 3D Plasmonic Cloaking in Free Space

David Rainwater*† and Aaron Kerkhoff‡
Applied Research Laboratories, The University of Texas at Austin, Austin, TX 78758-4423, USA

Kevin Melin
Dept. of Physics and Dept. of Electrical and Computer Engineering, The University of Texas at Austin, Austin, TX 78712, USA

Andrea Alù§
Dept. of Electrical and Computer Engineering, The University of Texas at Austin, Austin, TX 78712, USA

(Dated: July 20, 2011)

We report the first experimental verification of a metamaterial cloak for a 3D object in free space. We apply the plasmonic cloaking technique, based on scattering cancellation, to suppress microwave scattering from a finite dielectric cylinder. We verify that scattering suppression is obtained all around the object and for different incidence angles, validating our measurements with analytical results and full-wave simulations. Our experiment confirms that realistic and robust plasmonic metamaterial cloaks may be realized for elongated 3D objects at microwave frequencies.

The use of metamaterials to achieve electromagnetic (EM) cloaking has been the focus of intense investigation in the past decade (see *e.g.* Refs. [1, 2] for reviews of the various approaches). Numerous techniques have been proposed to divert or suppress EM scattering, using exotic properties of several classes of metamaterials. From the theoretical standpoint, several of these approaches have successfully proven that metamaterial layers are in principle very effective at drastically reducing, even totally suppressing, the total scattering [3, 4]. However, experimental realization has so far been very limited: the available experimental proof-of-concept EM cloaks have been restricted to waveguides and 2D geometries [5, 6]; or to "carpet cloaks", which only hide bumps on perfect reflectors [7, 8]. The real goal of cloaking – in fact its very definition – is to make an object undetectable at all angles and for all forms of excitation.

Here we report what we believe is the first successful experimental demonstration of a 3D cloak in free space. Our test object is a finite-length elongated cylinder. We apply the "plasmonic cloaking" technique [9], which has shown theoretical promise for robust isotropic response. It is enabled by the anomalous scattering features of thin plasmonic layers with low or negative effective permittivity, which can yield drastic scattering cancellation via local negative polarizability [9, 10].

The literature on metamaterial cloaking of cylinders has so far dealt mostly with idealized 2D geometries: infinite cylinders, incident waves normal to the cylinder axis, and specific polarizations. Our recent work [11] instead analyzed finite-length effects and excitation at oblique incidence. We showed that plasmonic metamaterial shells can minimize scattering even under these conditions. We further emphasized the importance of considering the coupling between transverse-magnetic (TM_z) and transverse-electric (TE_z) polarizations at oblique incidence, which plays a significant role in the cloak design and operation. Nevertheless, our numerical simulations gave a very positive outlook for large scattering reduction over reasonable bandwidths and broad range of incidence angles for cylinders with moderately large cross section and length comparable to the incident wavelength. However, in Ref. [11] we analyzed only ideal homogeneous metamaterial layers from the theoretical standpoint.

Our present analysis is dedicated to the design, realization and testing of a real metamaterial plasmonic cloak to suppress microwave scattering off a dielectric cylinder. We show good comparison between theory and experiment for various incidence angles, including monostatic and bistatic measurements. Our results pave the way to the realization of 3D stand-alone cloaks for radar evasion and non-invasive radio frequency (RF) probing [12].

The object to be cloaked is a circular dielectric cylinder of length L, radius a, permittivity ϵ and permeability μ. We begin by first designing an idealized plasmonic cloak using the theory described in [9, 10]; this is a thin cylindrical shell of thickness $(a_c - a)$ with homogeneous permittivity ϵ_c and permeability μ_c. Even though plasmonic cloaks may be arbitrarily thin, we selected a thickness 30% of the cylinder radius ($a_c/a = 1.3$) so as to simplify manufacturing and allow use of commercially-available high permittivity dielectric materials. Our design is optimized for total scattering reduction of TM_z polarization at normal incidence, as TM_z is the dominant scattering polarization for dielectric cylinders of moderate cross

*corresponding author
†Electronic address: rain@arlut.utexas.edu
‡Electronic address: kerkhoff@arlut.utexas.edu
§Electronic address: alu@mail.utexas.edu

section, and normal incidence has the highest total scattering width. We consider a metamaterial design with non-magnetic properties and a single-layer cloak, so the only design parameter is the cloak effective permittivity, ϵ_c. (As a practical matter this choice excludes the cloaking of conducting cylinders, which require magnetic properties [11].) Following our theoretical results, single-layer plasmonic cloaks require negative permittivity, ϵ_c, to achieve robust scattering suppression.

Next, we develop a physical metamaterial cloak design to realize the required effective permittivity. Negative effective permittivity values, $\epsilon_c < 0$, may be obtained in the microwave range using various metamaterial geometries, such as wire media or parallel-plate implants [13]. In particular, the parallel-plate technology may be particularly well-suited for cloaking incident TM_z waves, as shown for normal incidence in Ref. [14]. This concept was also used to experimentally verify cloaking of a dielectric rod inside a waveguide [5], making the experiment effectively a 2D validation for scattering cancellation at normal incidence [5].

Here, we extend this approach to finite cylinders illuminated by TM_z plane waves at arbitrary oblique angles in free space. The design requires length-spanning metallic strips extending radially outward from the core, embedded in a high-density substrate of permittivity ϵ_s; cf. Fig. 1. For normal incidence and TM_z polarization of wavenumber k_0, the effective permittivity of the cloak follows a Drude dispersion model [14]:

$$\frac{\epsilon_c}{\epsilon_0} \;=\; \epsilon_s \;-\; \frac{(N/2)^2}{(k_0 a)^2}\;. \qquad (1)$$

It is evident that the cloak's performance in terms of isotropy is better for a larger number of strips, N; but this comes at the price of higher substrate permittivity to keep ϵ_c (1) at a near-zero value, ideal for cloaking purposes [9]. Critically important are the inner and outer radial gaps, w_i and w_o, between the metallic strip longitudinal edges and the cloak surfaces, as well as the strip thickness, as discussed in Ref. [14]. The strips, or fins, effectively operate as waveguide plates slightly below cutoff at the desired frequency, creating an effective low negative permittivity for the dominant mode. A finite fin thickness shortens the effective waveguide height, slightly detuning the operating frequency. This may be compensated in practice by increasing the strip edge gaps. For oblique TM_Z incidence, the dominant waveguide mode is unperturbed, implying that the normal component of the electric field is shorted by the metallic fins. This produces a strong spatial dispersion mechanism for ϵ_c, analogous to wire medium [15] or slit metamaterials [16]. As our simulations show, however, these effects are negligible in our cloak design, due to the short fin length.

The test cylinder and cloak shell are both made of machined Cuming Microwave C-Stock dielectric material. To simplify fabrication, we constructed the cloak shell as an assembly of segments as depicted in Fig. 1 rather than as a solid piece of dielectric with embedded strips. The strips in this case were precision-cut copper tape applied to one face of each segment, such that the proper edge gaps are obtained upon assembly. The segments are held together with thin end caps, which are made of low permittivity Teflon so as to minimally impact the EM signature of the test cylinder / cloak combination.

We designed the cloaked cylinder to exhibit scattering suppression at $f_c = 3$ GHz. The characteristics of our test cylinder to be cloaked are $L = 18$ cm, $a = 1.25$ cm, and $\epsilon = 3\epsilon_0$. Its length is slightly less than two wavelengths at the design frequency, to avoid axial wave resonances that may be observed in simulations of longer cylinders, due to traveling waves. Optimized cloak permittivity is $\epsilon_c = -13.6\epsilon_0$, from the theory derived in Ref. [11], neglecting spatial dispersion effects for oblique incidence in our metamaterial realization. Using the design equations of Refs. [5, 14] as a starting point and refining the design parameters with simulation, our cloak is constructed of 8 dielectric segments with permittivity $\epsilon_s = 16\epsilon_0$. The copper tape used for the metallic strips has thickness 0.066 mm, separated from the inner core by an optimized $w_i = 0.98$ mm, and from the outer core by $w_o = 1.3$ mm. Fig. 1 shows the practical realization of the cloak components and assembled cloaked cylinder.

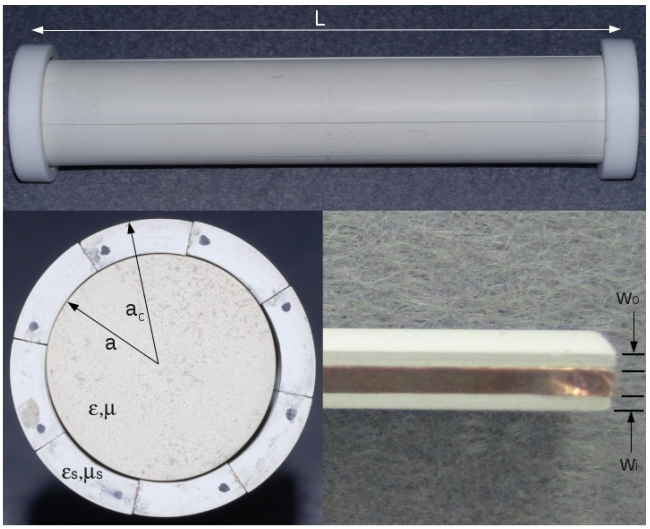

FIG. 1: Photographs of: (top) the assembled cloak on the test cylinder with end caps; (bottom left) a cross-section view of the assembly with end cap removed; (bottom right) a shell segment edge with copper tape used to form the metallic strip for the metamaterial cloak.

We performed a series of far-field scattering measurements to determine the monostatic and bistatic radar cross section (RCS), σ, of the cloaked cylinder. Our non-anechoic laboratory environment necessitated vector background subtraction and software-based time gating steps in post-processing to remove background clutter, as described below. The target was placed on a styrofoam block 1.4 m from each of two calibrated ETS-Lindgren 3115 ultra-wideband double-ridged waveguide horn antennas, connected to an Agilent 8719ES vector network

analyzer (VNA). We measured the raw complex scattering response between the two antennas as the scattering parameter $\mathbf{S_{21}}$. Repositioning the antennas about the target at constant target distance achieved the desired monostatic or bistatic orientation.

Background subtraction requires two measurements: one with the target in place, yielding $\mathbf{S_{21,T}}$; another with only the target removed, yielding $\mathbf{S_{21,B}}$. The quantity $\mathbf{S_{21,S}} = \mathbf{S_{21,T}} - \mathbf{S_{21,B}}$ closely corresponds to the response of the target with most environmental effects removed. Software-based time gating further reduces clutter. This processing step is expressed as:

$$\mathbf{S'_{21,S}} \;=\; fft\{\mathbf{W} \cdot ifft\{\mathbf{S_{21,S}}\}\} \qquad (2)$$

where $fft\{\}$ and $ifft\{\}$ are the fast Fourier transform and its inverse, and $\mathbf{W}$ is a rectangular window function used to gate out returns due to background clutter.

Post-processed S-parameter measurements are converted to RCS values using the radar range equation:

$$|\mathbf{S'_{21,S}}|^2 \;=\; \frac{P_r}{P_t} \;=\; \frac{G_t G_r \lambda^2 \sigma}{(4\pi)^3 R_t^2 R_r^2} \qquad (3)$$

where P_r (P_t) is the received (transmitted) power, G_t (G_r) is the transmit (receive) antenna gain, λ is the free space wavelength, and R_t (R_r) is the distance between the target and transmit (receive) antenna. Substituting measured and known values (including antenna gain calibration values), one can solve for σ.

To achieve high temporal resolution in the time gating step, measurements were performed over a wide frequency band, 1 to 5 GHz. This procedure was repeated for the dielectric test cylinder both with and without the metamaterial cloak applied. The difference in $\mathbf{S'_{21,S}}$ between the two measurements yields the scattering gain.

We performed simulations using both CST Microwave Studio and Ansoft HFSS for comparison with measurements. The two simulation codes were found to give nearly identical results; thus, only the CST curves are presented for clarity. For brevity, we present graphical results only for select incidence angles, and only for the window 2.5–3.5 GHz. Our numerical simulations consider the realistic metamaterial design, but neglect the complex measurement apparatus and post-processing, which explains part of the minor disagreements between simulated and experimental results.

Fig. 2 shows results for monostatic scattering gain for polar incidence angles, $\theta = 90°$ (normal) to $\theta = 30°$. Overall, good agreement between measurement and simulation is achieved for each incidence angle and over the full range of frequencies. Strong scattering suppression around the design frequency $f_0 = 3$ GHz is predicted by numerical simulation and verified by experiment, confirming that the permittivity model (1) is accurate also for oblique incidence and that cloaking may be realistically achieved as predicted in Ref. [11]. A suppression of ≥ 9.8 dB is seen for each incidence angle. The small variations in the frequency at which scattering suppression occurs as a function of incidence angle, present in both measurement and simulation, is well-predicted by our theoretical calculations; it is associated with the TM–TE polarization coupling for incidence angles away from normal [11]. Though not shown for conciseness, we found that the cloak provided very limited scattering suppression for grazing angles ($\theta \approx 0$), which agrees with our predictions [11]. We stress, however, that this scenario is not so relevant for practical purposes, since the cross section and total scattering is much smaller for small θ.

Although measurement and simulation trends agree well, small differences appear. The small frequency shifts at which scattering gain peaks and troughs occur are most likely due to manufacturing and assembly imprecision. The reduced variation in measured scattering gain near the peaks and troughs as compared with simulation is likely due to a combination of test object imperfections, the complex measurement apparatus, and the time gating step in measurement processing, which reduces frequency resolution somewhat. Nonetheless, these results show that backscatter can be strongly suppressed for several different positions of the excitation and observer. We believe that even better agreement may be obtained in an anechoic or open environment.

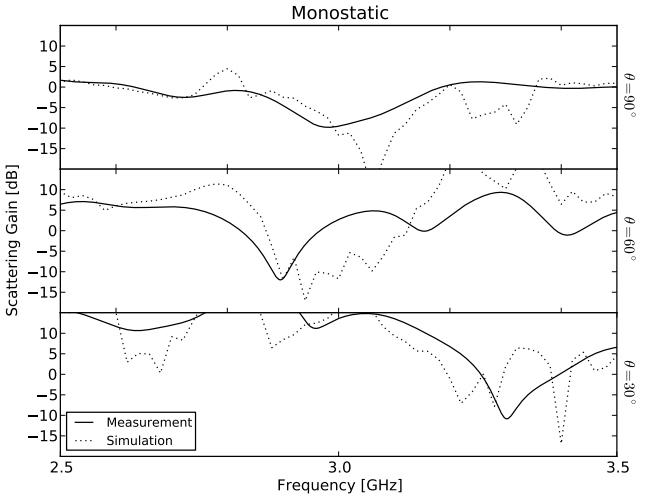

FIG. 2: Monostatic scattering gain [dB], cloaked cylinder relative to uncloaked, for various incidence angles as labeled: measurement (solid) and simulation (dotted).

Bistatic results are even more interesting, since they show that substantial scattering reduction may be obtained for all observer positions and arbitrary excitation. We divide them into two subgroups. The first subgroup consists of measurements scanning over polar angle, θ, for fixed azimuth angle, ϕ, between emitter and collector, shown in Fig. 3. The second subgroup, the curves of Fig. 4, is a scan over azimuthal angle for fixed polar angle. In both cases, measurement and simulation exhibit good overall agreement. For nearly every bistatic orientation, strong suppression, ≥ 7.6 dB, is exhibited in measurement near the design frequency. The exception to this

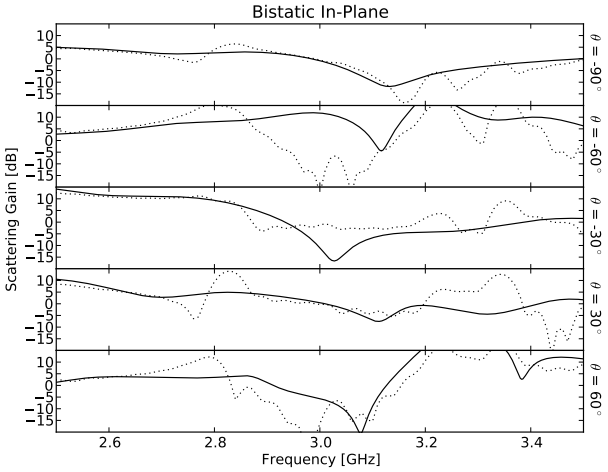

FIG. 3: Bistatic scattering gain [dB], cloaked cylinder relative to uncloaked, for normal incidence at $\phi = 0$ and various polar angles: measurement (solid) and simulation (dotted.)

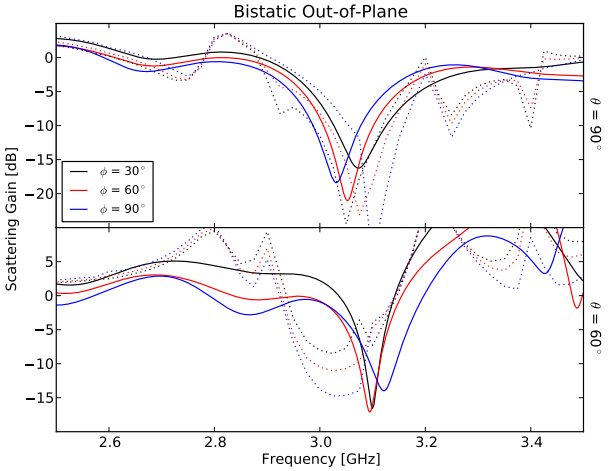

FIG. 4: Bistatic scattering gain [dB], cloaked cylinder relative to uncloaked, for several choices of incidence angle as labeled: measurement (solid) and simulation (dotted.)

is ($\theta = -60°$, $\phi = 0°$) where the measured suppression (4.4 dB) is lower than predicted by simulation. This may again be due to manufacturing and assembly imprecision, which causes the cloaking frequency response to narrow.

The similarity of azimuthal-variation curves in Fig. 4 demonstrates isotropic response, as predicted by our theoretical model [11] and the weak relevance of spatial dispersion effects due to the chosen metamaterial geometry. Variation over polar angle (Fig. 3) is less isotropic, as expected, but strong suppression is still observed over a wide range of angles, independently varying the excitation and observations positions, again consistent with our theoretical expectations.

To conclude, we have presented the first experimental demonstration of a 3D stand-alone cloak in free space, applying the plasmonic cloaking technique to a finite circular cylinder approximately two wavelengths long, illuminated by microwave radiation. Our results show that robust and strong scattering suppression can be obtained at the frequency of interest and over a moderate frequency range, weakly dependent on the excitation and observer positions. Experimental measurements closely match theoretical predictions and numerical simulations. Scattering may be strongly reduced even for large incidence angles and near-grazing incidence. These concepts may be extended to infrared and optical wavelengths using alternative realizations of plasmonic metamaterials. The design chosen here limited the ultimate thinness of our cloak. We are currently exploring an alternative realization using the mantle-cloaking technique [17], which may further reduce the overall cloak thickness.

Acknowledgments

A. A. was partially supported by the National Science Foundation (NSF) CAREER award ECCS-0953311. A. K., K. M. and D. R. were supported by an internal research award at ARL:UT. We thank Joel Banks of ARL:UT for the developing the mechanical implementation of the parallel-plate metamaterial.

[1] P. Alitalo and S.A. Tretyakov, *Mat. Today* **12**, 212 (2009).
[2] A. Alù and N. Engheta, *J. Opt. A* **10**, 093002 (2008).
[3] J. B. Pendry, D. Schurig and D. R. Smith, *Science* **312** 1780 (2006).
[4] G.W. Milton, N.A. Nicorovici, R.C. McPhedran and V.A. Podolskiy, *Proc. Roy. Soc. Lond.* **461**, 3999 (2005).
[5] B. Edwards, A. Alù, M.G. Silveirinha and N. Engheta, *Phys. Rev. Lett.* **103**, 153901 (2009).
[6] D. Schurig *et al.* , *Science* **314**, 977 (2006).
[7] T. Ergin *et al.* , *Science* **328**, 337 (2010).
[8] B.-I. Popa, L. Zigoneanu and S. A. Cummer, *Phys. Rev. Lett.* **106** 253901 (2011).
[9] A. Alù and N. Engheta, *Phys. Rev. E* **72**, 016623 (2005).
[10] A. Alù and N. Engheta, *Phys. Rev. E* **78**, 045602 (2008).
[11] A. Alù, A. Kerkhoff and D. Rainwater, *New J. Phys.* **12**, 103028.
[12] A. Alù and N. Engheta, *Phys. Rev. Lett.* **102**, 233901 (2009).
[13] W. Rotman, *IRE Trans. Antennas Propag.* **10**, 82 (1962).
[14] M.G. Silveirinha, A. Alù and N. Engheta, *Phys. Rev. E* **75**, 036603 (2007).
[15] P.A. Belov *et al.* , *Phys. Rev. B* **67**, 113103 (2003).
[16] A. Alù, G. D'Aguanno, N. Mattiucci and M. Bloemer, **Phys. Rev. Lett. 106**, 123902 (2011).
[17] A. Alù, *Phys. Rev. B* **80**, 245115 (2009).